Review of Commercial SiC MOSFET Models: Topologies and Equations

Andrii Stefanskyi, Łukasz Starzak, Andrzej Napieralski
Department of Microelectronics and Computer Science
Lodz University of Technology
Łódź, Poland
andrii.stefanskyi@p.lodz.pl

***Abstract*—SPICE models of silicon carbide power MOSFETs provided by manufacturers currently present on the market have been compared. Model subcircuit topologies have been identified and described. Principal equations have been extracted and related to common MOSFET models.**

***Keywords*—modeling, MOSFET, SiC, SPICE**

I. Introduction

In the recent years, silicon carbide (SiC) power MOSFETs have been introduced to the market. They have the advantages of much lower on-resistance (than silicon MOSFETs), faster switching speed (than IGBTs) and higher maximum operating temperature. They are able to improve the properties of power converters, but an optimal design requires reliable and precise electro-thermal models.

There are different approaches and mathematical models to reproduce electrical and thermal behaviour of MOSFETs. In this respect, models of four different transistors supplied by all the commercial device manufacturers currently present on the market were investigated: SCT20N120 from STMicroelectronics (further referred to as ST model), C2M0160120D and C3M0065090D from Cree (C2M and C3M model, respectively) and SCT2160KE by ROHM (ROHM model).

In Section II, the identified components and connections within model subcircuit topology will be briefly described. Mathematical relationships realised by behavioural components and extracted from SPICE model codes will be analysed in Section III. Sections IV and V will cover the parts of the models responsible for dynamic and thermal behaviour, respectively. Finally, conclusions will be formulated in Section VI.

II. Model Structures

Model structures were determined by building circuit schematics that correspond to component and connection descriptions given in model source SPICE codes. The general approach common for all the analysed models is to describe device behaviour with analogue behavioural modelling (ABM) components: controlled current and voltage sources with arbitrary equations. Fig. 1 presents obtained model structure. ABM sources are displayed without equations.

It can be seen that the ST model (Fig. 1 a) has the most complex topology. Also, code description of this model is organised linearly in one single block. Similar code structure is used in the ROHM model, but it contains less components (see Fig. 1 d). To the contrary, models proposed by Cree (Figs. 1 b and c) have hierarchic code structure: the die block is represented by a subcircuit and so are parasitic capacitances. Despite its simple schematic topology, the C3M model code is relatively complicated due to fitting functions used and the high number of their parameters (55).

III. Static Behaviour Modelling

A. Forward Characteristic

As described in [5], the ST model is based on the well-known LEVEL1 MOS model which describes the behaviour of the surface of the semiconductor under the influence of an electronic field. The difference between the ST model and the standard LEVEL1 [6] consists in the presence of two additional temperature-dependent coefficients V_{lin} and KP_{sat} that adjust forward and reverse drain-source currents according to

$$I_{DS} = \begin{cases} A \cdot V_{DS}(1+\lambda V_{DS})\left(V_{GS} - V_{th} - \frac{V_{DS}}{2}\frac{V_{lin}}{KP_{sat}}\right)V_{lin} \\ \text{for } V_{DS} < (V_{GS} - V_{th})\frac{KP_{sat}}{V_{lin}} \\ A \cdot (1+\lambda V_{DS})(V_{GS} - V_{th})^2 KP_{sat} \\ \text{for } V_{DS} > (V_{GS} - V_{th})\frac{KP_{sat}}{V_{lin}} \end{cases} \quad (1)$$

where V_{GS} and V_{DS} are gate and drain voltages, V_{th} is threshold voltage, T_j is junction temperature, A is area and λ is channel length modulation parameter.

While the ST model uses a single voltage-controlled current source (VCCS) component, marked in Fig. 1 a as *Gmos*, the C2M model uses two VCCS (*G1* and *G2* in Fig. 1 b) realising two logarithmic functions to interpolate between two regions of operation in order to obtain a single-piece modified Enz-Krummenacher-Vittoz (EKV) MOSFET model [7]. The original EKV model has been improved by adding curve fitting parameters to match SiC specificity and to include the effect of channel length modulation [8], yielding

This paper is part of the ADvanced Electric Powertrain Technology (ADEPT) project which is an EU funded Marie Curie ITN project, grant number 607361.

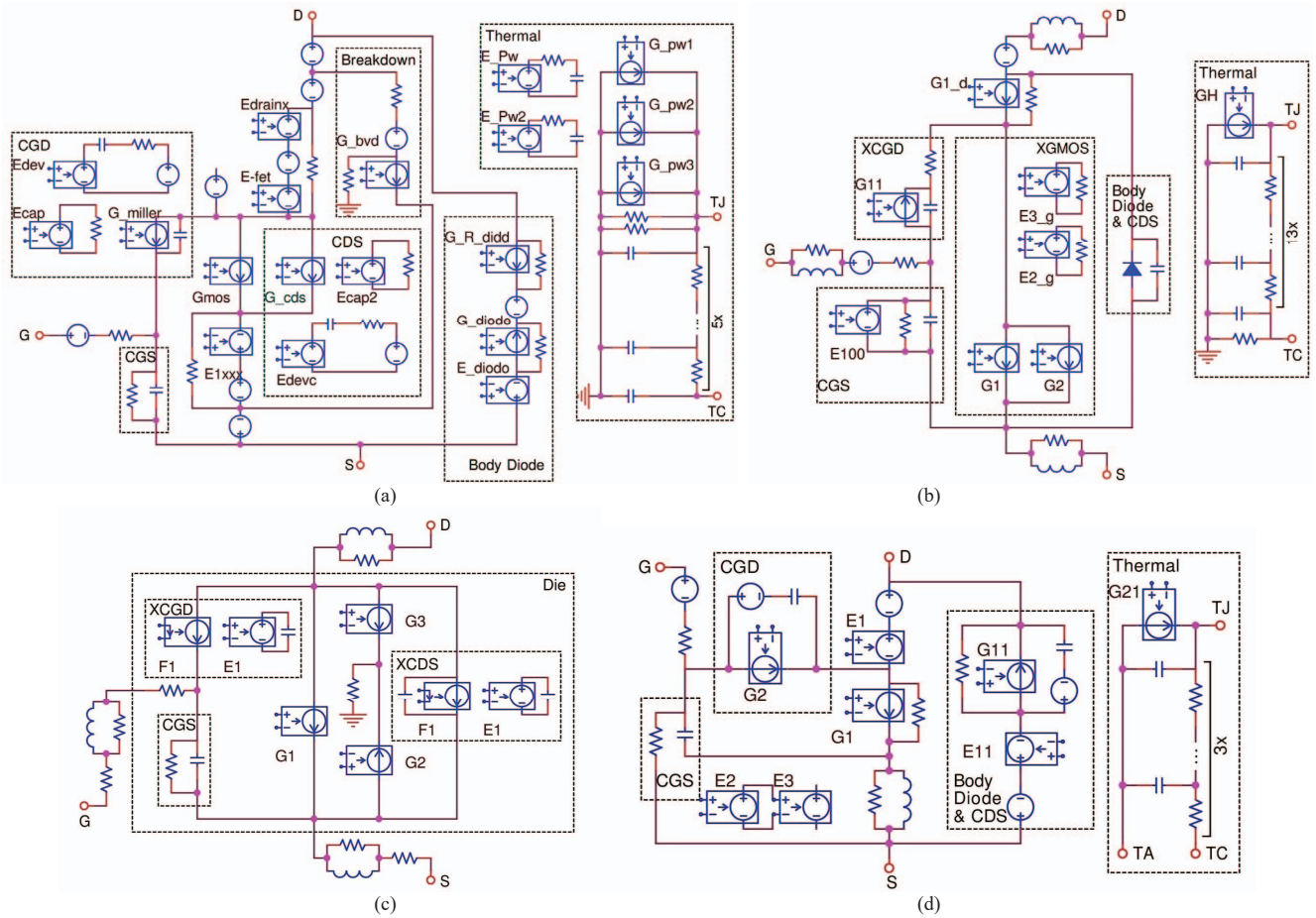

Fig. 1. Simplified electrical schematics (dependent source inputs and some ground connections omitted) for (a) ST, (b) C2M, (c) C3M and (d) ROHM models

$$I_{DS} = 2g_m\phi_t^2 k_s \left\{ \left[\ln\left(1 + \mathrm{e}^{\frac{V_{GS}-V_{th}}{2k_s\phi_t}}\right)\right]^k - \left[\ln\left(1 + \mathrm{e}^{\frac{(V_{GS}-V_{th})-nV_{DS}^a}{2k_s\phi_t}}\right)\right]^k \right\}(1+\lambda V_{DS}) \quad (2)$$

where ϕ_t is thermal voltage, g_m is transconductance; k_s is sub-threshold slope parameter, k is law exponent and a and n are triode region parameters.

Transconductance and threshold voltage in the C2M model are implemented respectively by the *E2_g* and *E3_g* voltage sources (Fig. 1 b) which implement the temperature dependences of these parameters. Also, in series with the drain-source current components, there is the *G1_d* VCCS that models a temperature-dependent resistance described with:

$$I_{D2D1} = \frac{V_{D2D1}}{A_1 \cdot {T_j}^2 + A_2 \cdot T_j + A_3 + 10^{-9}} \quad (3)$$

where I_{D2D1} and V_{D2D1} are current and voltage across the resistance, A_1, A_2 and A_3 are constant parameters.

The Curtice-Ettenberg FET model [9] with additions and modifications has been used by Cree to describe its third generation devices (C3M). The channel current equation of the C3M model is implemented by *G1* in Fig. 1 c and it includes separately the effects of gate and drain voltages on the *I-V* characteristics:

$$I_{DS} = \frac{{k_{ah}(\mathrm{T}_j)\cdot V_{GS}}^{k_{ae}(\mathrm{T}_j)+a}}{\left({V_{GS}}^{2\cdot b}+\mathrm{e}^{2\cdot c}\right)^d \cdot \left[{V_{GS}}^{2k_{af}(\mathrm{T}_j)}+\mathrm{e}^{2k_{af}(\mathrm{T}_j)k_{ag}}\right]^{\frac{k_{ae}(\mathrm{T}_j)}{2k_{af}(\mathrm{T}_j)}}} \cdot \tanh(\gamma V_{DS})(1+\lambda V_{DS}) \quad (4)$$

where V_{GS} and V_{DS} are the internal gate and drain voltages, γ is slope adjustment parameter, $k_{ah}(\mathrm{T}_j)$, $k_{ae}(\mathrm{T}_j)$, $k_{af}(\mathrm{T}_j)$ are temperature-dependent coefficients and k_{ag}, a, b, c, d are temperature-independent coefficients.

The differences between (4) and the original Curtice model mostly concern the gate-related part: (4) doesn't use quadratic or cubic polynomial interpolation and it includes temperature dependence. Moreover, the γ parameter in the C3M model is dependent on V_{GS} and on temperature.

The approach used in the ROHM model is similar to Curtice and EKV models in that the drain current is modelled by a single VCCS, *G1* (Fig. 1 d), and that its formula contains a V_{GS} and a V_{DS}-related component, which can be presented as:

$$I_{DS} = f_g(V_{GS}) \cdot f_d(V_{DS}) \quad (5)$$

where $f_g(V_{GS})$ and $f_d(V_{DS})$ describe gate and drain voltage effect relationships given by:

$$f_g(V_{GS}) = V'_{GS} \cdot \left[1 + \left(B_1 + B_2 \cdot \tanh\left(\frac{V'_{GS}}{c_1}\right)\right) \cdot \frac{e^{\frac{T_j - T_0}{-c_T}}}{10}\right] \quad (6)$$

$$f_d(V_{DS}) = \frac{V_{DS}}{|V_{DS}| + \left(B_1 + B_2 \cdot \tanh\left(\frac{V'_{GS}}{c_1}\right)\right) \cdot e^{\frac{T_j - T_0}{-c_T}}} \quad (7)$$

where B_1, B_2, c_1, c_T are constant parameters, and V'_{GS} is an implicit function of V_{GS} and T_j:

$$V'_{GS} = G_1 \cdot V''_{GS}{}^{\left[g_t \cdot \exp\left(\frac{T_j - T_0}{g_1}\right) \cdot \exp\left(\frac{T_j - T_0}{g_2}\right) \cdot \exp\left(\frac{T_j - T_0}{g_3}\right)\right]} \quad (8)$$

with $V''_{GS} = f(V_{GS}, V'_{GS}, T_j)$ and G_1, g_t, g_1, g_2, g_3 are constants.

In the ROHM model, the on-state resistance is modelled with a current-controlled voltage source (CCVS, *E1* in Fig. 1 d) connected in series with the drain-source current VCCS. This resistance influences both forward and reverse characteristics and its equation is

$$V_D = D_1 \cdot I_D \cdot e^{\frac{Tj - T_0}{d_1} e^{\frac{Tj - T_0}{d_2}}} + D_2 \cdot I_D \cdot |I_D|^k \cdot e^{\frac{Tj - T_0}{d_3}} \quad (9)$$

where V_D and I_D are drain voltage and current, D_1, D_2, d_1, d_2, d_3 and k are constant parameters, and T_0 is nominal temperature.

All the four models include thermal relationships. However, it can be noted that their mathematical form is much different in each case.

B. Reverse Bias

For all the analysed models, the common feature in describing device behaviour under reverse bias is the use of components that represent the body diode, which follows directly from the power MOSFET semiconductor structure. Together with this common part, reverse static characteristic calculation for ST and C2M models also includes the drain-source current equation (1) and (2), respectively. To the contrary, drain-source current equations (4) and (5) of C3M and ROHM models describe only their forward behaviour.

The body diode ST model consists of two VCCS, *G_R_didd* and *G_diode* (Fig. 1 a), that represent diode resistance and diode current behaviour, the latter expressed with:

$$I_{diode} = e^{-15 + \frac{V_{diode}}{a_1 - a_2 \cdot e^{-6} \cdot T_j}} - B \quad (10)$$

where I_{diode} and V_{diode} are current and voltage across the diode, a_1, a_2 and B are constant parameters.

The C2M model structure (Fig. 1 b) contains an internal body diode model in the form of a standard SPICE diode component connected in parallel to the series connection of the drain-source current VCCS (*G1* and *G2*) and the drain resistance *G1_d*.

In the case of the C3M model, the reverse behaviour is achieved using two VCCS, *G2* and *G3* (see Fig. 1 c), connected in series. They represent a gate voltage-dependent resistance and a diode-like component, described with

$$I_{DD1} = \frac{1}{a \cdot [f_{hyp}(V_{GS})]^2 + b \cdot f_{hyp}(V_{GS}) + c} \cdot V_{DD1} \quad (11)$$

where V_{GS} is gate-source voltage, V_{DD1} is voltage across the resistance component and a, b, c are temperature-dependent coefficients; and

$$I_{D1S} = \left[f_{hyp}(V_{SD1})\right]^{f_{kbb}(V_{G1S}, T_j)} \cdot e^{f_{kaa}(V_{G1S}, T_j)} \quad (12)$$

where V_{SD1} is reverse drain-source voltage and $f_{kbb}(V_{G1S}, T_j)$ and $f_{kaa}(V_{G1S}, T_j)$ are functions of gate-source voltage including temperature dependences. The function $f_{hyp}(x)$ is given by:

$$f_{hyp}(x) = \frac{x + \sqrt{x^2 + 4 * (1e^{-6})^2}}{2} \quad (13)$$

In the ROHM model, the body diode is also modelled with two components representing diode resistance and diode current behaviour. However, in this case, they are a CCVS and a VCCS (*E11* and *G11* in Fig. 1 d), respectively. The latter is defined with a complex formula that will be referenced again in Section IV:

$$\begin{aligned} I_{diode} = {} & A_1 \cdot \left\{\exp\left[\frac{V_{diode}}{a_1 \cdot \exp\left(\frac{T_j - T_0}{-b_1}\right)}\right] - 1\right\} \cdot \\ & \cdot \exp\left[\frac{T_j - T_0}{-b_2} \cdot \exp\left(\frac{T_j - T_0}{b_3}\right)\right] \cdot (1 + \exp(-V_{diode} - \\ & - A_2 \cdot \frac{\exp\left(\frac{T_j - T_0}{b_4}\right)}{A_3})) + \frac{dV_{diode}}{dt} \cdot \\ & \cdot \left[B_1 \cdot (V_{diode} - B_2) + B_3 \cdot \left(1 - c_1 \cdot \frac{\tanh\left(\frac{V_{diode}}{c_1}\right)}{c_2}\right)^{-c_3}\right] \end{aligned} \quad (14)$$

where V_{diode} and I_{diode} are voltage and current across the body diode, respectively; A_1 through A_3, B_1 through B_3, a_1, b_1 through b_4 and c_1 through c_3 are constant parameters.

As it can be seen, the C3M and ROHM models contain many constant parameters without any clear physical interpretation. Due to their high number, it is supposed that their extraction can only be done numerically.

IV. Parasitic Capacitances

The gate-to-drain and drain-to-source capacitances of a power MOSFET are voltage-dependent [10]. In the C3M model, this is achieved using a voltage-controlled voltage source (VCVS) *E1* (see Fig. 1 c) with a capacitor producing voltage derivative over time, and a current source realising the capacitor equation including its voltage dependence:

$$i_{cap} = C(v_{cap}) \cdot \frac{dv_{cap}}{dt} \quad (15)$$

where i_{cap} and v_{cap} are capacitance current and voltage, respectively.

A similar topology is found in the ST model, but with a separate VCVS (*Ecap* and *Ecap2* in Fig. 1 a) realising the $C(v_{cap})$ function through a look-up table. Also, the capacitance realisation found in the ST model includes additional VCVS (*Edev* and *Edevc* in Fig. 1 a) that reproduce junction temperature (T_j) values as well as two VCCS, *G_miller* and *G_cds*, that introduce capacitance currents into the main subcircuit.

The C2M model explicitly implements only the C_{GD} variable capacitance using a single ABM current source, *G11* (Fig. 1 b), to realise (15) including both voltage derivation and the $C(v_{cap})$ function. A hyperbolic tangent function is applied to approximate the latter. The voltage-dependent C_{DS} is included in the standard SPICE diode model representing the body diode. A constant capacitor is added in parallel, representing the capacitance value for high voltages.

In the ROHM model, C_{GD} is implemented similar to the C3M model; it contains a VCCS, *G2* (Fig. 1 d), however without an additional VCVS. On the other hand, C_{DS} is included in the body diode ABM current source, which can be seen in (14) as the voltage derivative term.

Each of these approaches has different consequences for compatibility with different SPICE-based simulators. The voltage-dependent capacitance embedded in the standard diode component as found in the C2M model, is compatible with any SPICE version. On the other hand, where (15) is explicitly implemented through an ABM source formula (ROHM model), it requires a derivative-over-time function to be available. The C3M has lower requirements as a standard capacitor is used to produce this derivative. A look-up table feature is required for the ST model.

As the gate-to-source parasitic capacitance C_{GS} does not change with terminal voltages [10], it is represented by a single standard SPICE capacitor component in all the analysed models.

V. Thermal Part

Three of the considered models (ST, C2M and ROHM) include a thermal part together with electro-thermal coupling. It is a distributed model making use of the mathematical equivalence between the electrical and thermal domain provided that a linear heat conduction model is assumed. The equivalent electrical circuit for the heat conduction path is composed of several RC couples whose number varies considerably between models: from 3 in ROHM to 14 in C2M. The electro-thermal coupling is realised by calculating the dissipated power and feeding it to the thermal circuit with a current source representing thermal power; junction temperature, equal to the voltage across this source, is then fed back to the electrical part through equations of the ABM components.

Power dissipation is modelled in different ways. In the C2M model, there is one ABM current source (*GH* in Fig. 1 b) summarizing the power produced in the drain-source and one produced in the gate-source circuits. The ST model has three sources (*G_pw1*, *G_pw2* and *G_pw3* in Fig. 1 a) calculating the power generated by the drain-source current, the power dissipated in the body diode current and the power connected with avalanche breakdown. In the ROHM model, there is one ABM source (*G21* in Fig. 1 d) that uses an arithmetical sum expression to yield power dissipation in the drain circuit, including the body diode, as well as in the gate circuit.

Unlike the rest of the revised models, a thermal part is absent from the C3M model. As such, it does not allow self-heating effects into account or to design a cooling system.

VI. Conclusions

From the presented analysis it is clear that each manufacturer's approach is similar in that all models have the form of sub-circuits containing ABM components (with the exception of the body diode in the C2M model). As such, they can only be used with SPICE versions offering the analogue behavioural modelling feature.

However, specific model subcircuit topologies are different not only for various manufacturers but also for consecutive technologies from a single manufacturer, such as the second and the third generation devices from Cree. Moreover, each of the considered models is based on a substantially different mathematical description of MOSFET behaviour: Level 1, EKV or Curtice. The ROHM could not be directly linked to any of the standard MOSFET models; nevertheless, it can be classified as similar to EKV and Curtice in some respects.

The purpose of this work was to investigate existing approaches to the modelling of silicon carbide power MOSFET transistors. The results of this analysis will be used in future work devoted to the development of a universal SiC MOSFET model that will be applicable to various devices present on the market.

References

[1] SCT20N120. Device datasheet. http://www.st.com/content/ccc/resource/technical/document/datasheet/c6/f3/b3/4d/4d/80/47/14/DM00118513.pdf/files/DM00118513.pdf/jcr:content/translations/en.DM00118513.pdf.

[2] C2M0160120D. Device datasheet. http://www.wolfspeed.com/media/downloads/169/C2M0160120D.pdf.

[3] C3M0065090D. Device datasheet. http://www.wolfspeed.com/media/downloads/176/C3M0065090D.pdf.

[4] SCT2160KE. Device datasheet. http://www.rohm.com/web/global/datasheet/SCT2160KE.

[5] G. Bazzano, D.G. Cavallaro, R. Greco, A. Raffa, and P.P. Veneziano, "A new analog behavioral SPICE macro model with thermal and self-heating effects for Silicon Carbide power MOSFETs," Proceedings PCIM Europe, Nuremberg, Germany, 2015, pp. 1-8.

[6] G. Massobrio and P. Antognetti, Semiconductor device modeling with SPICE. New York: McGraw-Hill, 1993.

[7] Y.S. Chauhan, F. Krummenacher, and A.M. Ionescu, "Modeling of high voltage MOSFETs based on EKV (HV-EKV)," in Power/HVMOS Devices Compact Modeling, W. Grabinski and T. Gneiting, Eds. Dordrecht: Springer, 2010, pp. 95-127.

[8] B.N. Pushpakaran, S.B. Bayne, G. Wang, and J. Mookken, "Fast and accurate electro-thermal behavioral model of a commercial SiC 1200V, 80 mΩ power MOSFET," 2015 IEEE Pulsed Power Conference (PPC), Austin, TX, 2015, pp. 1-5.

[9] S. Maas, "Fixing the Curtice model," Microwave J., March, 2002.

[10] V. Benda, J. Gowar, and D.A. Grant, Power Semiconductor Devices. Chichester: Wiley, 1999.